Boundary-Layer Meteorol (2006) 118: 379–400
DOI 10.1007/s10546-005-0608-y

ON THE TURBULENCE IN THE UPPER PART OF THE LOW-LEVEL JET: AN EXPERIMENTAL AND NUMERICAL STUDY

L. CONANGLA[1,3,*] and J. CUXART[2]
[1]*Dept. Física Aplicada, Universitat Politècnica de Catalunya, Manresa, Spain;* [2]*Grup de Meteorologia, Dept. Física, Universitat de les Illes Balears, Spain;* [3]*Dept. Física Aplicada, Escola Universitària Politècnica de Manresa, Av. de les Bases 61-73, 08240 Manresa, Catalunya, Spain*

(Received in final form 2 December 2004)

Abstract. The characteristics of low-level jets (LLJ) observed at the "Centro de Investigacion de la Baja Atmósfera" (CIBA) site in Spain are analysed, focussing on the turbulence generated in the upper part of the jet, a feature that is still to be thoroughly understood. During the Stable Boundary Layer Experiment in Spain (SABLES) 1998, captive balloon soundings were taken intensively, and their analyses have highlighted the main characteristics of the jet's wind and temperature structure, leading to a composite profile. There are indications that the turbulence has a minimum at the level of the wind maximum, with elevated turbulence in a layer at a height between two and three times that of the LLJ maximum, but no direct measurements of turbulence were available at these heights. In September 2001, a 100-m tower at the same site was re-instrumented to give turbulence measurements up to 96.6 m above ground level. All occurrences of LLJ below this height between September 2002 and June 2003 have been selected and significant turbulence above the LLJ has been found. Simulations with a single-column turbulence kinetic energy model have been made in order to further investigate the generation of elevated turbulence. The results correlate well with the measurements, showing that in the layer above the LLJ, where there is significant shear and weakly stable stratification, conditions are conducive to the development of turbulence.

Keywords: Elevated turbulence, Low-level jet, Nocturnal boundary layer, SABLES 98, Stable boundary layer, Single-column model.

1. Introduction

At nighttime under clear-sky conditions and with weak synoptic winds, a wind maximum close to the ground can exist, often referred to as a low-level jet (LLJ). The maximum can exist for much of the night, with supergeostrophic winds. Several factors influence the formation and persistence of this coherent structure. The horizontal gradients of temperature imply a change of geostrophic wind with height, which may favour the formation of a low-level wind maximum. These temperature gradients can be related to differential heating on sloping terrain (Holton, 1967; Mahrt, 1981a), on heterogeneous terrain

* E-mail: laura@eupm.upc.edu

(Wu and Raman, 1997), or to the sea-land wind regime (Källstrand, 1998), among other factors.

On the other hand, the inertial oscillation can lead to supergeostrophic wind values (Blackadar, 1957), and to a LLJ. The mechanism proposed by Blackadar is most pronounced on the Great Plains of the U.S.A. (Zhong et al., 1996), although Whiteman et al. (1997) distinguished between a LLJ formed in this way and those associated with cold-air advection behind cold fronts.

The knowledge of wind behaviour at low levels, and in particular wind maxima, is important in wind energy applications and for the transport and dispersion of pollutants (Banta et al., 1998). Furthermore, enhanced vertical shear modifies air-surface exchange (Darby et al., 2002), and Arritt et al. (1997) and Wu and Raman (1998) found a correlation between wind maxima and severe storm events.

Several studies have suggested that the wind shear above the wind maximum can generate elevated turbulence, particularly in the layer above the temperature inversion (Mahrt et al., 1979; Smedman, 1988; Smedman et al., 1993), inducing a downwards transport of momentum, heat or scalars, that can be sporadic or intermittent (Smedman, 1988; Parker and Raman, 1993; Banta et al., 2002).

In our study we investigate the turbulence generated in the upper part of the LLJ. In Section 2, an analysis of the characteristics of the observed LLJ during the Stable Boundary Layer Experiment in Spain (SABLES 98; Cuxart et al., 2000b) is made, using available captive balloon soundings. Section 3 shows the analysis of the new data available from the same site for the period September 2002 to June 2003, where instrumentation on a 100-m tower operated continuously and provided high-frequency data at up to 96 m above ground level (a.g.l.), a height that is in some cases above the wind maximum. In Section 4, a study of the LLJ prototype for the site is made using a 1.5-order turbulence scheme. Finally, in Section 5, a summary and conclusions are given.

2. Low-level Jet in the SABLES 98 Experiment

2.1. Site characteristics and instrumentation

SABLES 98 experiment took place in September 1998 at the ''Centro de Investigacion de la Baja Atmósfera'' (CIBA, 41 °49′ N, 4°56′ W). The CIBA is located at the centre of the north Castillian Plateau (corresponding to the basin of the Duero river), on a smaller plateau known as Montes Torozos, which is a flat structure of 800 km^2 at 840 m above sea level (and approximately 50 m above the surrounding flat lands), where grains are grown. The Duero basin is surrounded by high mountain ranges, located approximately 100 km north,

east and south around the site, with the river flowing westwards to the sea (see Figure 1). The Torozos plateau has a gentle slope of 30 m along 50 km from the north-east to the south-west, and the north-west and south-east borders are slightly above the level of the inner plateau.

An intensive campaign of captive balloon soundings was performed using the AIR-3A tethersonde system, with a line of 1000 m, and the speed of ascent and descent controlled by a manual dial on the winch; the sensors include dry-bulb and wet-bulb thermistors, an aneroid capacitance barometer, a three-cup anemometer with tachometer and a magnetic compass; samples were obtained at a rate of one every 10 s. Furthermore, turbulence measurements on a 100-m tower were made, with high-frequency data up to a height of 32 m.

2.2. Observations

The week 14–21 September 1998 was ideal for stable boundary-layer measurements, since an anticyclone was fixed to the west of the Iberian Peninsula, with very weak horizontal pressure gradients at low levels and clear skies. A subsidence inversion was present at a height of 2000 m above sea level. The nights had an approximate duration of 12 h.

Classification of the stability for this period is made following the proposal of Mahrt et al. (1998), using sonic anemometer data at 5.8 m above the ground for the interval 1800-0600 UTC, computing z/L using 5-min averages, where z is the height and L is the Obukhov length. The value $z/L = 0.06$ separates the weakly stable regime from the moderately stable (or transitional) regime, and $z/L > 1$ defines the very stable regime. In Figure 2 the nightly z/L proportions of each category are given and it is seen that the moderate and strongly stable stratification predominate.

The captive balloon was operated continuously during this period, and 61 soundings are available. Forty-nine soundings have been used since they all reach at least a height of 400 m and many up to 800 m, with the first data point under 9 m a.g.l. (under 5 m in 88% of the soundings), with a vertical resolution between 1 and 7 m (at least in the first few metres in 86% of the soundings).

2.3. Soundings with a LLJ present

Twenty-eight of the forty-nine selected soundings (57%) show a well-defined LLJ, fulfilling the requirement (Stull, 1988; Andreas et al., 2000) that there be decreasing wind speed values of at least 2 m s^{-1} both upwards and downwards of the maximum, although Banta et al. (2002) used a value of 1.5 m s^{-1}. Here the value of 1.5 m s^{-1} has been retained for wind maxima below 40 m height, in order to avoid discarding interesting cases with maxima near the ground. In Figure 3 several wind speed profiles are shown corresponding to different days and hours; these profiles are typical of the whole dataset.

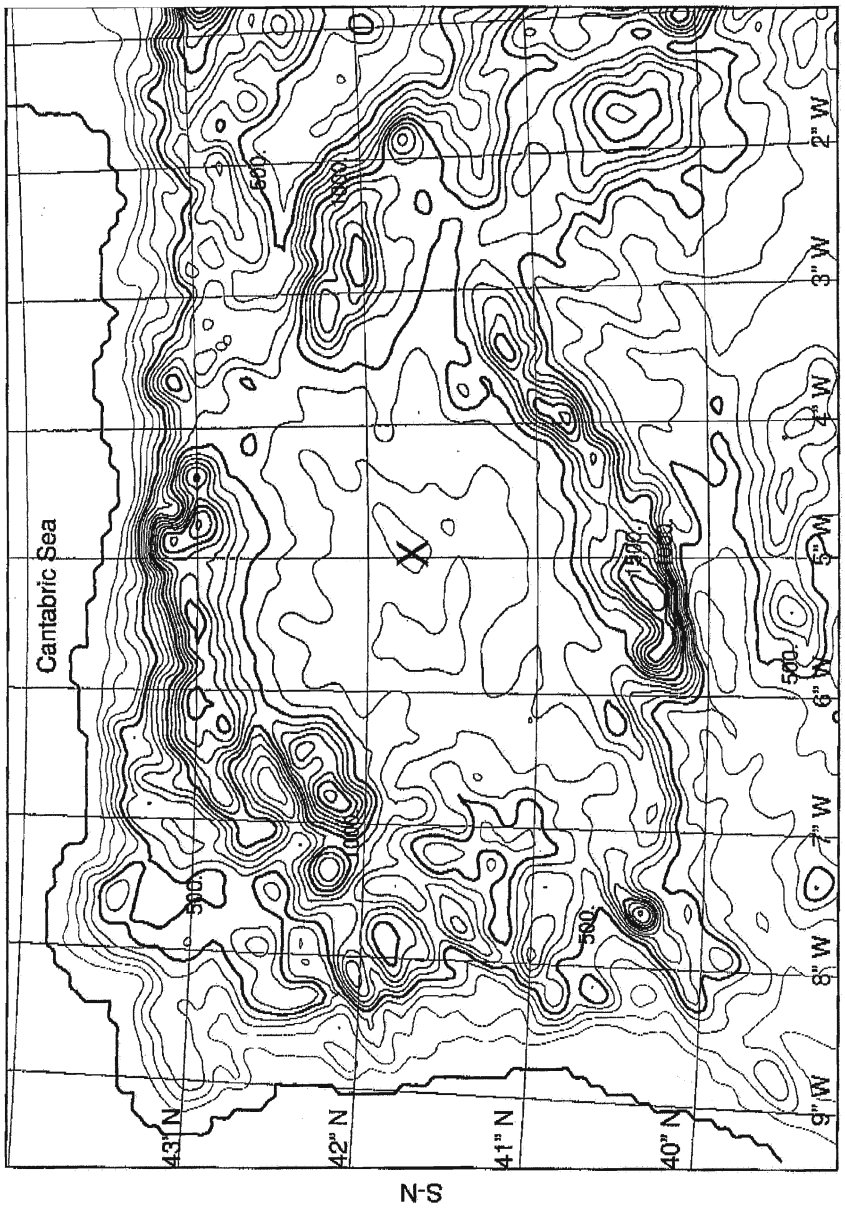

Figure 1. Orography of the north-western Iberian Peninsula, to 5-km resolution, generated with a digital land model. The location of the CIBA is indicated by a cross symbol (X).

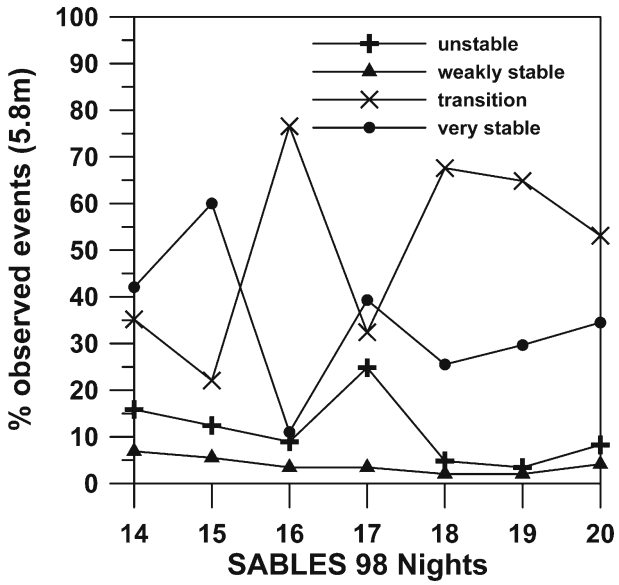

Figure 2. Proportion of each stability type, for the period 14–20 September 1998 during the SABLES 98 campaign, at a height of 5.8 m.

Some characteristics from these selected soundings are given in Figure 4. The height of the maxima is between 21 and 137 m, with 21.5% of cases between 80 and 90 m a.g.l.; the speeds vary between 3.5 and 11.5 m s^{-1}, with 25% having values between 7 and 8 m s^{-1}. Finally, the wind direction is from 25 and 125 degrees (north-north-east and east-south-east), but in up to 43% of cases it is from the east (between 80° and 100°) for the whole night. No significant correlations have been found for these variables studied in pairs.

In order to systematize the available information, a composite sounding has been constructed. To do so, the profiles have been normalized with respect to the height of the wind maximum (h_{LLJ}), and profiles with a vertical resolution of $0.1h_{\mathrm{LLJ}}$ have been produced for the 28 soundings. The averages and standard deviations are illustrated in Figure 5, for wind speed and direction, potential temperature (using the average surface pressure of the site, 920 hPa, as a reference value), Brunt-Väisälä frequency (N_{BV}) squared and the gradient Richardson number in finite differences. These have been defined as:

$$N_{BV}{}^2 \simeq \frac{g}{\bar{\theta}} \frac{\Delta \bar{\theta}}{\Delta z}, \tag{1}$$

$$Ri = \frac{\left(\frac{g}{\bar{\theta}} \frac{\Delta \bar{\theta}}{\Delta z}\right)}{\left(\frac{\Delta U}{\Delta z}\right)^2 + \left(\frac{\Delta V}{\Delta z}\right)^2}, \tag{2}$$

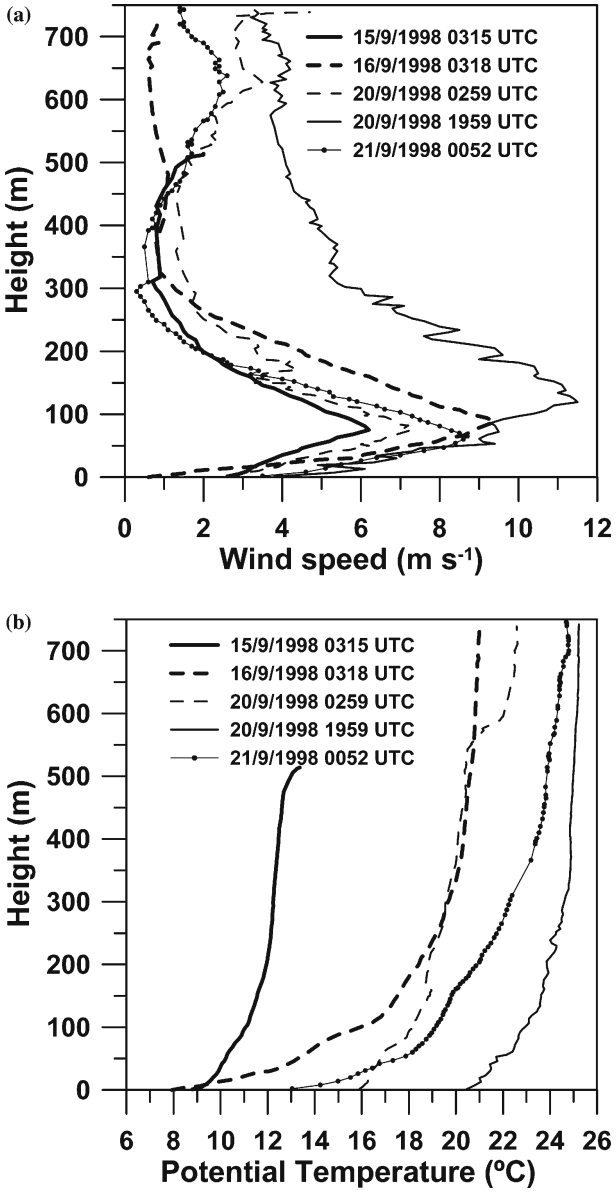

Figure 3. (a) Some wind speed profiles with a LLJ, from the balloon soundings made at CIBA during SABLES 98. (b) Potential temperature related to the same soundings.

where g is the gravity acceleration, $\bar{\theta}$ denotes mean potential temperature, and $\Delta\theta$, Δz and (ΔU, ΔV) are the increments in potential temperature, height and wind speed between the different observational levels.

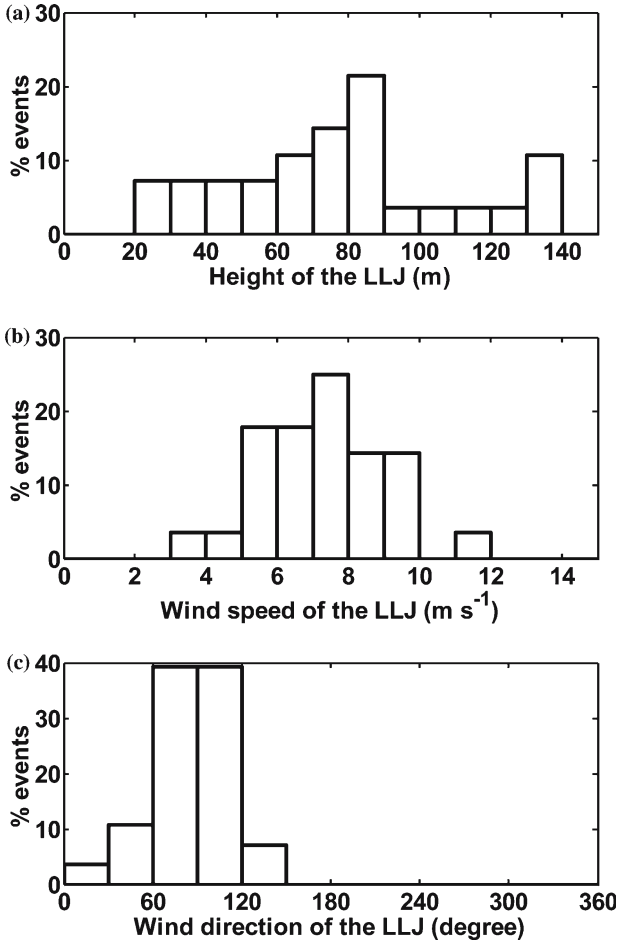

Figure 4. Histograms of height (a), speed (b) and direction (c) of the wind maxima. Data obtained from the selected LLJ profiles, of the balloon soundings made at CIBA during SABLES 98. Percentage of occurrences in each x-bin is shown along the vertical axis.

We consider the averaged profiles as the composite sounding (Figure 5); this has a wind maximum of 7.2 m s^{-1}, with values of 5.2 m s^{-1} (2 m s^{-1} less than the maximum) at $0.42h_{LLJ}$ and $1.77h_{LLJ}$ fulfilling the criterion we have used for the selection. The wind direction is from the east up to a height of more than $2.5h_{LLJ}$, indicating the likely orographic origin of this structure, since no evidence of an inertial oscillation is found.

The potential temperature profile shows a significant mean gradient just below the LLJ of approximately 2.3 K (the gradient dimensions are °C or K because z/h_{LLJ} is non-dimensional), and greater close to the ground ($\approx$3.6 K); at above $1.6h_{LLJ}$ the mean gradient is weaker and approximately constant

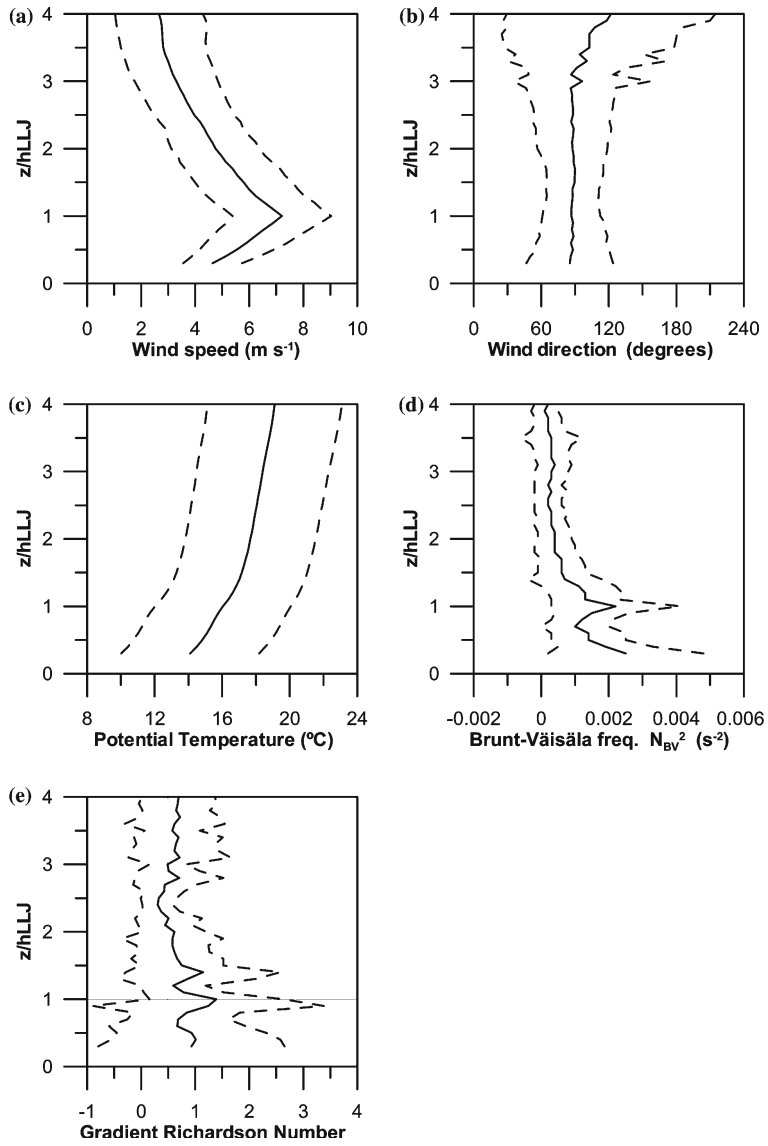

Figure 5. Composite profiles constructed from individual profiles with a LLJ, obtained from balloon soundings made at CIBA during SABLES 98. First, scaling the height with the jet height for each individual sounding, then interpolating values to levels every $0.1h_{\mathrm{LLJ}}$ and then averaging. Average (solid line) and standard deviation (dashed line) of wind speed (a), wind direction (b), potential temperature (c), squared Brunt-Väisälä frequency (d) and gradient Richardson number in finite differences (e).

with height (0.7 K). Mahrt et al. (1979) propose a value of around 1.4–$1.5h_{\mathrm{LLJ}}$ where this change of gradient occurs, very close to that found for the SABLES composite.

There is a slight change of curvature in the temperature profile at h_{LLJ}, which becomes evident in the N^2_{BV} profile, locating the larger values of stratification precisely at h_{LLJ} and close to the ground; just above $1.4h_{LLJ}$ the standard deviation of N^2_{BV} allows for the existence of non-stably stratified layers as marginal cases. The internal waves of higher frequency, according to this plot, would be confined to the layers very close to the ground and at the inversion located at h_{LLJ}.

It is customary to take a critical value of 0.5 or even larger for the gradient Richardson number in finite difference form (Mahrt, 1981b; Stull, 1988), and the average profile shows $Ri > Ri_c$ everywhere except in the layer between 2 and $3h_{LLJ}$. There is, however, a large scatter, and values well below critical can exist for the whole depth under study, with maximum variability near the ground, and minimum variability at the layer in question between 2 and $3h_{LLJ}$. The maximum value of Ri is at h_{LLJ}, where the strong vertical gradient of temperature coincides with the weakest wind gradient, therefore producing a layer with a small probability of sustained turbulence, as anticipated by Mahrt et al. (1979). Smedman et al. (1993) found similar results for a LLJ study over the Baltic Sea, including an estimate of the budget of the turbulence kinetic energy (TKE). It is shown that the minimum production of TKE is located at the height of the maximum wind speed, whereas the maximum is somewhere above, like most of the SABLES 98 individual soundings and the composite.

3. Experimental Evidence of Turbulence at the Upper Part of the LLJ

3.1. New instrumentation at the CIBA site and data selection

In the preceding section some indirect indications of turbulence at the upper part of the LLJ during the SABLES 98 experiment have been given, mostly using the gradient Richardson number computed from the captive balloon soundings. However, the large uncertainty associated with this quantity, as can be seen in the large standard deviation values, does not allow us to reach firm conclusions on the existence of turbulence above h_{LLJ}. Furthermore, the highest sonic anemometer was located at 32 m and no high-frequency turbulence measurements were taken above h_{LLJ}.

As of September 2001, the 100-m CIBA tower was fully re-instrumented, and sonic anemometers were installed at 5.6, 19.6, 49.6 and 96.6 m height, together with traditional measurements of wind at 2.2, 9.6, 34.6, 74.6 and 98.6 m and of temperature at 0.0, 2.3, 10.0, 10.5, 20.5, 35.5, 97.0 and 97.5 m, and moisture at 0.0, 10.0, and 97.0 m. Since the LLJ was often located below 96.6 and 49.6 m (location of the two highest sonic anemometers) during SABLES 98, the available data base is explored to identify significant events.

Data between 1800 UTC and 0600 UTC have been chosen and quality control performed. Variances and covariances have been computed using 5-min averages and then have been averaged over 30-min periods to reduce random flux sampling errors. All the conventional data have also been averaged over 30-min periods. A total of 6912 30-min averages have finally been used for the present analysis, corresponding to 288 days. However, no soundings are available, unlike in SABLES 98.

3.2. Selection of the wind maxima

Wind profiles have been constructed using 30-min average values from wind sensors at 2.2, 5.6, 9.6, 19.6, 34.6, 49.6, 74.6, 96.6 and 98.6 m a.g.l. Correct correspondence between the different types of wind sensors was checked beforehand. We found that there are a large number of situations with a wind maximum above 34.6 m with decreasing values at the top levels of the tower. In order to have occasions with turbulent data above the wind maximum, profiles with wind maxima at 34.6, 49.6 or 74.6 m height have been analysed, although several restrictions have been imposed:

(i) the wind speed at 2. 2 m must be below 2 m s^{-1}, to correspond with situations in SABLES 98;
(ii) the wind maximum must be more than 2 m s^{-1} greater than the 2.2-m value (up to 3 m s^{-1} if the maximum is at 74.6 m);
(iii) the wind at 98. 6 m must be at least 1 m s^{-1} smaller than the maximum (0.5 m s^{-1} if the maximum is at 74.6 m, due to the proximity of the levels).

These restrictions provide a subset of 33 profiles with wind maxima at 34.6 m, a subset of 89 profiles with wind maxima at 49.6 m, and a subset of 31 profiles with the maxima at 74.6 m. The number of profiles is low compared with the total available, but the characteristics of the selected profiles are very close to those studied in SABLES 98. In fact, all the selected profiles with persistent wind maxima correspond to a synoptic situation very similar to the dominant one in SABLES 98 – that is, a high pressure system over the Atlantic ocean, with its centre near the Iberian Peninsula. In most of the cases (77.1%), the wind maximum is formed by 0100 UTC or later (particularly, 40.5% of cases are in the period between 0300 and 0500 UTC).

3.3. Characteristics of wind profiles

Figure 6 shows the average wind speed profile and the standard deviations when the maximum is at 49.6 m height, with the wind value scaled by its maximum value. The deviation is small and the shape is well-defined. Profiles

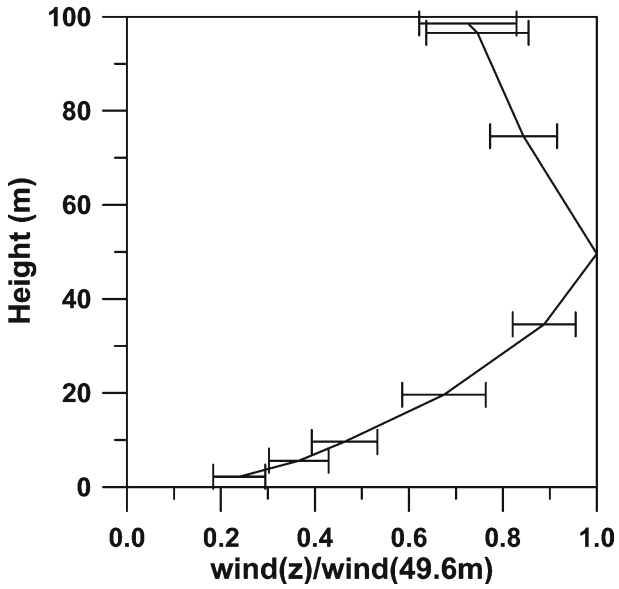

Figure 6. Average wind speed profile and standard deviation when there is a wind maximum at 49.6-m height. The wind profiles have been built using 30-min average values for all the levels where a wind sensor is available (2.2, 5.6, 9.6, 19.6, 34.6, 49.6, 74.6, 96.6 and 98.6 m height) at the 100-m CIBA tower (September 2002 to June 2003). The average wind profile has been computed from 89 selected shapes, showing a wind maximum at 49.6 m, with the wind value scaled by the maximum value.

have also been constructed for maxima at 34.6 and 74.6 m (not shown), and the results are very similar.

In Figure 7 the histograms of speed and direction of the wind maxima for the three levels together are shown. The wind speed is always below 9 m s^{-1} and above 4 m s^{-1} (the latter value by construction), whereas the predominant directions are between 30° and 180°, with more than 30% of cases between 60° and 90°, that is from the eastern direction, giving similar results as those found for the SABLES-98 experiment, but now with more occurrences from the south-east.

The thermal stability is computed using the criterion of Mahrt et al. (1998) as in Section 2, but now calculating the number of z/L occurrences in each stratification, from September 2002 to June 2003 with the presence of a selected wind maximum. The results are found in Table I, where it is clear that the moderate to strong stratification predominates for the selected cases.

3.4. Characteristics of the turbulence

The profiles of turbulence variables are studied for the selected cases. Table IIa gives the percentages at which the measurement of the turbulent

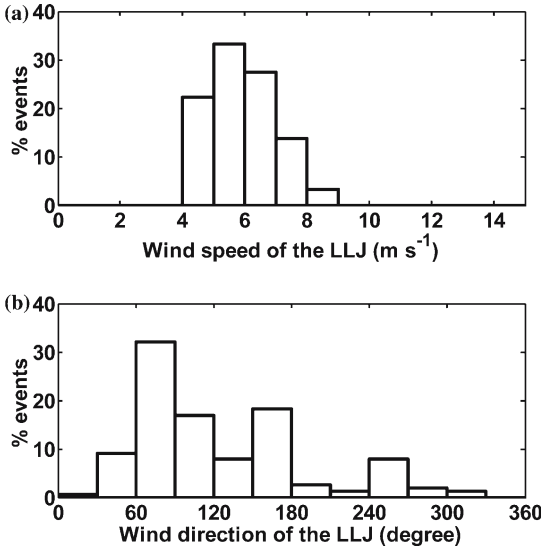

Figure 7. Histograms of speed (a) and direction (b) of the wind maxima, observed at 34.6-m, 49.6-m or 74.6-m height. 30-min average data were used, from the 100-m CIBA tower during the period September 2002 to June 2003. Percentage of occurrences in each x-bin is shown along the vertical axis.

kinematic heat flux ($-\overline{w'\theta'}$) is larger for every recording height. In general, the largest value is found close to the ground, although there are a significant percentage of cases (between 6.8 and 15.2%) where the largest value is found above the wind maximum. It is also interesting to note that the heat flux is never a maximum at the 49.6 m height where the wind maximum is located, suggesting that turbulence is weak in the nose of the wind maximum.

In Table IIb, the same computations are given for turbulence kinetic energy (TKE) and between 31.5% and 45.5% of the times the maximum is located above the wind maximum, therefore supporting the hypothesis of elevated turbulence above the LLJ, most likely due to the production by wind

TABLE I

Percentages of each stability type.

Maximum wind at height of:	Unstable	Weakly stable	Transition	Very stable
34.6 m	3.0	0.0	54.6	42.4
49.6 m	3.4	1.1	48.3	47.2
74.6 m	10.0	0.0	50.0	40.0

30-min average data at a height of 5.6 m were used from the 100-m CIBA tower during the period September 2002 to June 2003, when a wind maximum at 34.6-m, 49.6-m or 74.6-m height was observed.

TABLE II

(a) Percentages at which the measurement of turbulence kinematic heat flux ($-\overline{w'\theta'}$) is larger for every recording height. (b) Same as (a) except for turbulence kinetic energy.

(a) Maximum wind at:	Maximum kinematic heat flux ($-\overline{w'\theta'}$) is at height of:			
	5.6 m	19.6 m	49.6 m	96.6 m
34.6 m	66.6	18.2	6.1	9.1
49.6 m	49.4	43.8	0.0	6.8
74.6 m	48.4	32.2	9.7	9.7
(b) Maximum wind at:	Maximum TKE is at height of:			
	5.6 m	19.6 m	49.6 m	96.6 m
34.6 m	33.3	21.2	18.2	27.3
49.6 m	21.3	38.2	9.0	31.5
74.6 m	38.7	9.7	12.9	38.7

30-min average data were used, from the 100-m CIBA tower during the period September 2002 to June 2003, when a wind maximum at 34.6 m, 49.6 m or 74.6 m was detected.

shear. It is also interesting to note that the TKE is rarely a maximum at the wind maximum at (49.6 m) consistent with the idea that this layer has a minimum production of TKE by shear. When the wind maximum is at 34.6 m, the occurrence of the maximum TKE is greater at 96.6 m ($2.8h_{LLJ}$) than at 49.6 m ($1.4h_{LLJ}$), more or less consistent with the findings of Section 2 and the results of Smedman et al. (1993).

Let us now concentrate on those cases when the wind maximum is at 49.6 m, for the simple reason that this is the only level at which there is simultaneous wind and turbulence data. It has been seen that the kinematic heat flux ($-\overline{w'\theta'}$) at the first three levels (5.6, 19.6 and 49.6 m) diminishes with height in 43.8% of cases and never behaves in an upside-down manner; this is a pattern that is well in correspondence with a minimum of turbulence at h_{LLJ}. For the same analysis using turbulence kinetic energy, quite different results have been obtained: in 20.2% of cases the TKE behaves in a traditional manner and in 9.0% it is upside-down. Energy profiles do not behave as regularly as those of heat flux, and there are many cases with maximum or minimum TKE at the 19.6-m height; this is consistent with previous studies, such as Mahrt and Vickers (2003).

Concluding the analysis of turbulence data, the average profile of standard deviation of vertical velocity σ_w is shown in Figure 8, scaled by the 5.6-m value. The tendency is for minimum values at h_{LLJ} and to increase aloft, and in Figure 8a it is clear that a maximum value above the wind maxima occurs at the $2.8h_{LLJ}$ level.

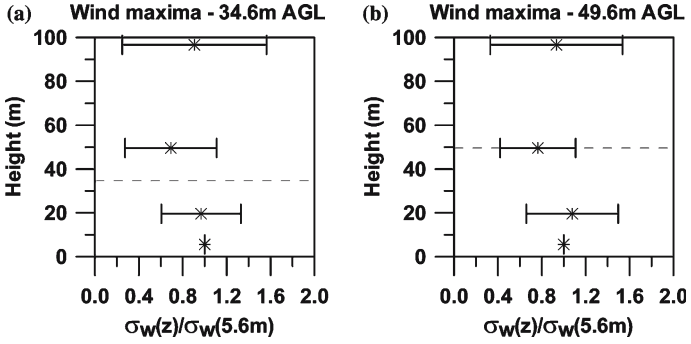

Figure 8. (a) Average and standard deviation of σ_w, scaled by its 5.6-m value. 30-min average values were used, from the 100-m CIBA tower during the period September 2002 to June 2003, when a wind maximum at 34.6-m was observed. The dashed line shows the wind-maximum height. (b) The same when a wind maximum at 49.6-m was detected.

4. Simulation of the LLJ with a TKE Single-column Model

4.1. The turbulence scheme

A 1.5-order turbulence scheme, described in Cuxart et al. (2000a), is implemented in the research numerical model Meso-NH (Lafore et al., 1998), in a three-dimensional (3D) implementation as a sub-grid model for large-eddy simulation, and in a one-dimensional (1D) implementation for mesoscale modelling. It is the basis for the scheme in the HIRLAM model (Unden et al., 2002), and it is used for fog forecasting in a single-column model used by the Spanish Weather Service (Terradellas and Cuxart, 2001).

In the 1D framework, the scheme uses the classical turbulence kinetic energy (e) evolution equation,

$$\frac{\partial e}{\partial t} = -\frac{\partial(\bar{w}e)}{\partial z} - \overline{u'w'}\frac{\partial U}{\partial z} - \overline{v'w'}\frac{\partial V}{\partial z} + \frac{g}{\bar{\theta}_v}\overline{w'\theta_v'} - \frac{\partial}{\partial z}\left(C_{2m} l e^{0.5}\frac{\partial e}{\partial z}\right) - C_\varepsilon \frac{e^{1.5}}{l}, \quad (3)$$

parameterizing the turbulence and pressure transport terms through a diffusion equation and expressing the dissipation term as a function of TKE and characteristic dissipation length (Kolmogorov, 1942). The same formulation is taken for both the transport and dissipation lengths (l).

As described in Cuxart et al. (2000a), fluxes derived from a complete second-order system are written, for a dry atmosphere,

$$\overline{u'w'} = -C_{MF} l e^{1/2}\frac{\partial U}{\partial z}, \quad (4)$$

$$\overline{v'w'} = -C_{MF} l e^{1/2} \frac{\partial V}{\partial z}, \tag{5}$$

$$\overline{w'\theta'} = -C_{HF} l e^{1/2} \frac{\partial \bar{\theta}}{\partial z} \phi_3, \tag{6}$$

where the function ϕ_3 plays the role of an inverse turbulence Prandtl number and, in a dry single-column framework, is given as a stability function;

$$\phi_3 = \frac{1}{1 + C_1 R_{1D}}, \tag{7}$$

$$R_{1D} = \left(\frac{g}{\theta_{vref}}\right) \frac{l^2}{e} \frac{\partial \bar{\theta}_v}{\partial z}. \tag{8}$$

The above constants are taken as: $C_{2m} = 0.40$, $C_\varepsilon = 0.70$, $C_1 = 0.139$, $C_{MF} = 0.067$, $C_{HF} = 0.167$.

The only free parameter is the turbulence mixing length, l. Following Bougeault and Lacarrère (1989), this is computed as the free path of a particle upwards (l_{up}) and downwards (l_{down}) considering that its initial energy is the turbulence kinetic energy of the starting level, and that it can travel until this energy is completely lost against the background buoyancy field or until it reaches the ground. In the present scheme, a unique length is computed for both the mixing and the dissipation.

The formulation reduces to a proposal of Deardorff (1980) for stable layer, except for a constant,

$$l = \sqrt{\frac{2e}{\frac{g}{\theta_{vref}} \frac{\partial \theta}{\partial z}}}. \tag{9}$$

Finally, the mixing length is computed as:

$$l_\varepsilon = \sqrt{l_{up} l_{down}}. \tag{10}$$

This proposal has been tested for dry convectively-driven atmospheric boundary-layer regimes in Cuxart et al. (2000a), and its extension in the cloudy planetary boundary layer (PBL) in Sánchez and Cuxart (2004). Its application for the strongly stably stratified PBL by Vukelic and Cuxart (2000) and Conangla et al. (2002) showed satisfactory behaviour, but for a weakly stable case such as the first GABLS (GEWEX Atmospheric Boundary Layer Studies, a program of the Global Energy and Water Cycle Experiment of the World Meteorological Organization; Holstlag, 2003) intercomparison (Cuxart et al., 2005) and for neutrally stratified flows it overestimates mixing and requires a limitation on the maximum values allowed.

In this study, the near-surface measured turbulent fluxes are taken as lower boundary conditions, and a simple longwave radiation scheme is applied (Pielke, 2002).

The horizontal structure of the boundary layer is introduced through external dynamic forcings, estimated from a mesoscale model, using pressure gradient, horizontal advection and mass divergence, which allows us to estimate the vertical velocities (Terradellas and Cuxart, 2001).

4.2. Analysis of a stationary LLJ

We have selected the period 0035-0445 UTC of the night of 20–21 September 1998 of the SABLES 98 experiment for a quasi-stationary model simulation. The average surface-layer kinematic heat flux was -5.7×10^{-3} K m s^{-1}, with a friction velocity 0.08 m s^{-1}. The synoptic and mesoscale advection estimated from the operational Spanish HIRLAM models was very weak. Three captive balloon soundings are available for this period, launched at 0052 UTC, 0157 UTC, 0258 UTC respectively, with very similar characteristics: wind maxima of 8–9 m s^{-1} at around 65 m a.g.l., from the east with a gentle turning clockwise in time. The potential temperature profile reveals a strong inversion near the ground and a change of gradient above, with approximate values of 7.9×10^{-2} K m^{-1} and 8.4×10^{-3} K m^{-1}, respectively for the 0052 UTC sounding; some layering developed later.

The initial profiles for the simulation are those from the 0052 UTC sounding (Figure 3); we perform a 3-h simulation run, using a time step of 10 s and a vertical resolution of 10 m. Mesoscale and synoptic advection is not taken into account. Average observed vertical surface fluxes are imposed and a geostrophic wind (2 m s^{-1}, direction 100°) is taken. The behaviour of the simulation during the first half hour is almost insensitive to the values of the geostrophic wind, and the spin-up of the model takes place in the first 10 min. Therefore we will first analyse here the period of 15–30 min after the start to avoid the influence of varying the geostrophic wind, and we will analyse in the next section the sensitivity to this parameter.

In Figure 9a it can be seen that the main features of the LLJ are reproduced. The model provides vertical profiles of the turbulence magnitudes such as the fluxes (Figure 9b) or the TKE budget (Figure 9c), thus complementing the information given by the soundings. Two distinct turbulent layers are shown separated by a minimum at the level of the wind maximum. The lower layer extends from the ground to the wind maximum, with diminishing values with height, in a way that could be described as traditional, although a secondary maximum is present above 30 m, where

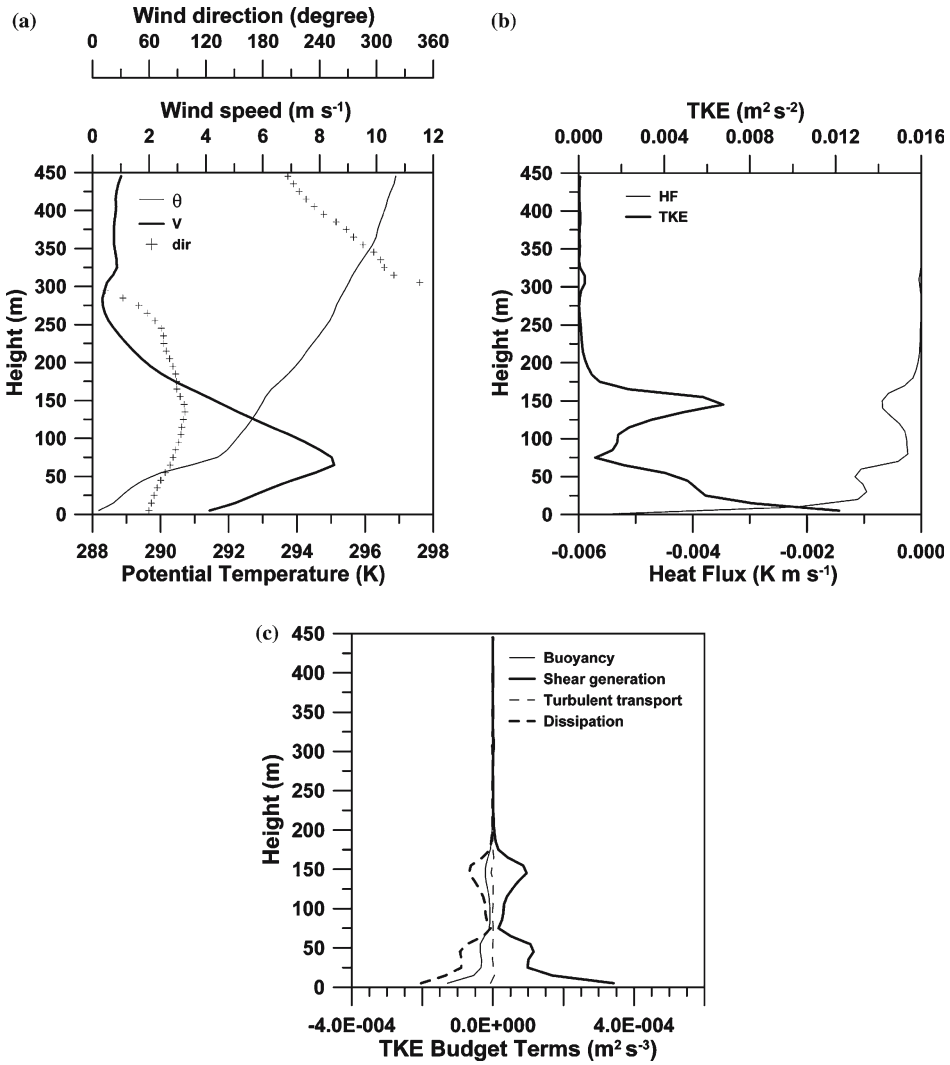

Figure 9. (a) Profiles of potential temperature, wind speed and wind direction, (b) kinematic heat flux, turbulence kinetic energy and (c) budget terms as seen in the model. The initial profiles for the simulation are those from the 0052 UTC sounding (Figure 3). Average results for the period 15–30 min after initiation are shown here.

evidence of layering seems to exist. The model links the heat flux to the TKE, and the corresponding heat flux profile basically follows TKE characteristics, a fact that is not always found in observations, and that might be seen as a limitation for TKE models.

The upper layer extends from the wind maximum to about 200 m with significant turbulence, a layer with stronger wind shear and weaker stability

than the underlying one. The largest TKE value is at approximately 145 m, which is 2.2 times the height of the wind maximum. This description fits well with the observations corresponding to lower LLJ from the tower and indications given by the gradient Richardson numbers from the soundings.

The turbulence (Figure 9c) is generated by wind shear in the entire column and the destruction is due to dissipation (around 70%) and negative buoyancy (around 30%). Here the buoyancy contribution is significantly larger than that for a weakly stable case, such as the first GABLS intercomparison exercise. The vertical turbulent transport is small for the whole column. All the described features are very similar to those we have mentioned regarding Smedman et al. (1993) for a LLJ over the Baltic Sea.

4.3. Sensitivity to the prescribed geostrophic wind

When a longer simulation is made, the results become sensitive to variations in the prescription of the geostrophic wind (v_g) at low levels (see Figure 11). A realistic simulation after 3 h is obtained through a prescription of a change with height of v_g as seen in Figure 10 – case 1. (A vertical variation of 4 m s^{-1} in the layer between 150 and 350 m a.g.l is taken, consistent with the thermal wind associated with the climatologically observed temperature difference across the northern Duero basin). The final profiles are quite stationary for the wind and temperature and have enhanced turbulence in the upper part of the LLJ. If v_g is considered constant with height, the wind maximum is kept but the main consequence is the progressive loss of the shear above the wind

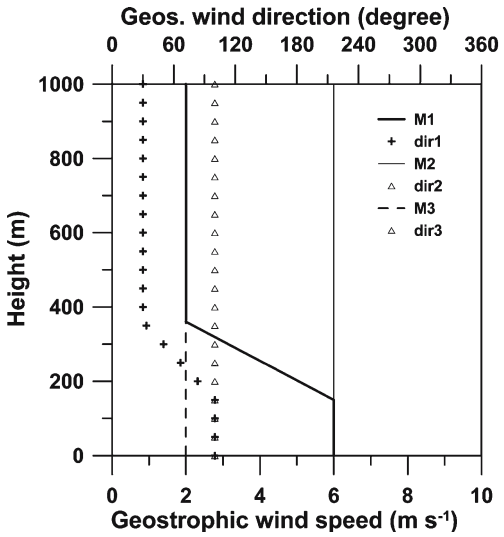

Figure 10. Speed and direction of the geostrophic winds used in the simulations.

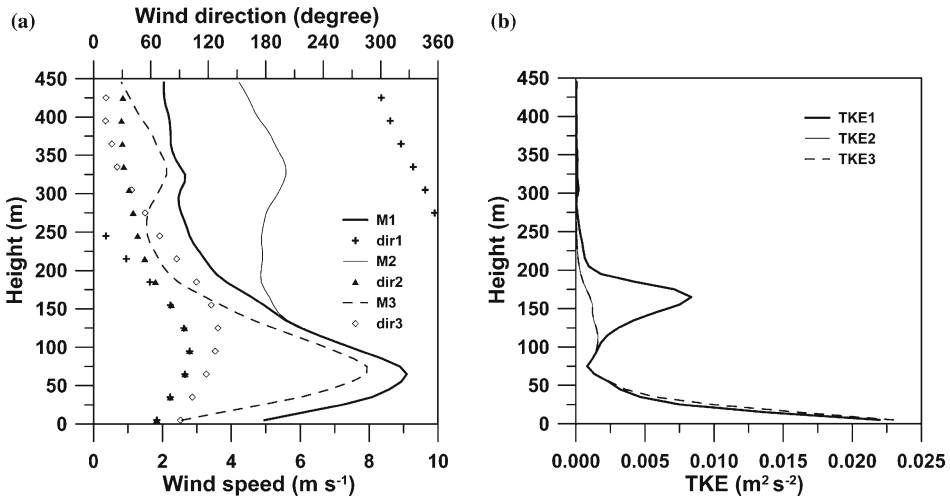

Figure 11. (a) Simulated profiles of wind speed and wind direction and (b) turbulence kinetic energy using different pressure gradients. The initial profiles for the simulation are those from the 0052 UTC sounding (Figure 3); the imposed geostrophic winds are seen in Figure 10. Average results for the period 2 to 3 h after initiation are shown here.

maximum. It seems that the model needs this vertical variation (module and/or direction) of v_g to sustain in time the turbulence in the upper part of the LLJ. Since v_g is a measure of the horizontal pressure gradient, it is likely that the pressure field near the surface is different from that at higher levels, due to local effects, in a way that an adjustment layer between the two layers might partially explain the modelled feature.

The prescription of v_g at the beginning of the night is also a key factor for the formation of the LLJ. Starting with a neutral profile at sunset it is necessary to impose a vertical variation on v_g to generate a LLJ, which might also as well support the hypothesis of the influence of local effects in the formation of the observed feature in the CIBA site. Once the LLJ is formed, its evolution is as described above for the stationary case.

5. Summary

The study of captive balloon soundings from the SABLES 98 experiment showed that LLJs are often observed at the CIBA under certain synoptic conditions. Their characteristics include a wind maximum between 21 and 137 m, with 21.5% of cases between 80 and 90 m, a maximum speed in the 3.5 to 11.5 m s^{-1} range, with 25% of cases between 7 and 8 m s^{-1}, and a direction varying between 25° and 125°, with 43% of cases in the 80–90° range, without evidence of any inertial oscillation.

A composite profile has been constructed from the ensemble of cases, using the height of the wind maximum (h_{LLJ}) as a normalizing quantity. It has a wind direction from the east at up to $2.5h_{LLJ}$, and a strong vertical temperature gradient close to the ground. At h_{LLJ} there is a significant change in the strength of stratification, and at $1.6h_{LLJ}$ stratification is very weak. At h_{LLJ} the Brunt-Vaisala frequency is a maximum and turbulence is minimal, whereas at the layer between 2 and $3h_{LLJ}$ there is a minimum value for the Richardson number, indicating the likely presence of elevated turbulence.

Observations from the re-instrumented tower at the CIBA site, during September 2002 to June 2003, have been explored to study similar events to those detected in SABLES 98, since continuous turbulence measurements are available for up to 96.6 m height. LLJs with heights equal to or lower than 74.6 m have been analysed for conditions similar to those found in SABLES 98 and observations indicate that the turbulence is minimal at h_{LLJ} and that there is elevated turbulence at the upper part of the LLJ, usually greater at $2.8h_{LLJ}$ than at $1.4h_{LLJ}$. Observations also indicate that the heat flux profile is more regularly varying with height than TKE or momentum flux profile.

To extend the study of the upper part of the LLJ, a simulation using a TKE model has been made. The run based on an observed stationary case out of the SABLES 98 database has shown that there is sustained turbulence at the level of interest, generated by strong shear together with weakly stable stratification. The results are qualitatively similar to the observations, although the simulation provides TKE and heat and momentum fluxes more coupled than in reality.

For a prognostic run, the formation and maintenance in time of elevated turbulence require a vertical variation of the geostrophic wind. This feature might be justified by vertical variation of the pressure field with height, since, close to the ground, local effects modify the field in respect to the layers above. Nevertheless, the origin of the LLJ at the CIBA is still an open question that should be further studied through high resolution mesoscale simulations in order to better determine the forcings at play in the process.

Acknowledgements

This study has been partially funded by the Spanish government through projects CLI97-0343, CLI98-1479E and REN2002-00486. We thank Prof. J.L. Casanova, director of CIBA, his kindness for the access to the site and to the data, Larry Mahrt and Maria Rosa Soler have given very useful ideas, Blazenka Vukelic and Enric Terradellas contributed to some stages on the development of the model, Manel Bravo worked on the preparation of the CIBA data set, and Maria Antònia Jiménez, Toni Mira and Lluís Fita have helped us much in obtaining information and some drawings.

References

Andreas, E. L., Claffey, K. J., and Makshtas, A. P.: 2000, 'Low-level Atmospheric Jets and Inversion over the Western Weddell Sea', *Boundary-Layer Meteorol.* **97**, 459–486.

Arritt, R. W., Rink, T. D., Segal, M., Todey, D. P., and Clark, C. A.: 1997, 'The Great Plains Low-level Jet during the Warm Season of 1993', *Mon. Wea. Rev.* **125**, 2176–2192.

Banta, R. M., Senff, C. J., White, A. B., Trainder, M., McNider, R. T., Valente, R. J., Mayour, S. D., Alvarez, T. M. H. R. J., Parrish, D., and Fehsenfeld, F. C.: 1998, 'Day-Time Buildup and Nightime Transport of Urban Ozone in the Boundary Layer during a Stagnation Episode', *J. Geophys. Res.* **103**, 22519–22544.

Banta, R. M., Newsom, R. K., Lundquist, J. K., Pichugina, Y. L., Coulter, R. L., and Mahrt, L.: 2002, 'Nocturnal Low-Level Jet characteristics over Kansas during CASES-99', *Boundary-Layer Meteorol.* **105**, 221–252.

Blackadar, A. K.: 1957, 'Boundary Layer Wind Maxima and their Significance for the Growth of Nocturnal Inversions', *Bull. Amer. Meteorol. Soc.* **38**, 282–290.

Bougeault, P. and Lacarrère, P.: 1989, 'Parameterization of Orography-induced Turbulence in a Mesobeta-Scale Model', *Mon. Wea. Rev.* **117**(8), 1872–1890.

Conangla, L., Cuxart, J., and Terradellas, E.: 2002, One-column Simulations of the SBL Observed during SABLES-98: Importance of the Surface Fluxes and the Dynamic Forcings', Preprints *15th Symposium on Boundary Layers and Turbulence*, Wageningen, The Netherlands, July 15–19: (2002) American Meteorological Society, 45 Beacon St., Boston, MA, pp. 313–314.

Cuxart, J., Bougeault, P., and Redelsperger, J. L.: 2000a, 'A turbulence Scheme Allowing for Mesoscale and Large-eddy Simulations', *Quart. J. Roy. Meteorol. Soc.* **126**, 1–30.

Cuxart, J., Yagüe, C., Morales, G., Terradellas, E., Orbe, J., Calvo, J., Fernández, A., Soler, M. R., Infante, C., Buenestado, P., Espinalt, A., Joergensen, H. E., Rees, J. M., Vilà, J., Redondo, J. M., Cantalapiedra, I. R., and Conangla, L.: 2000b, 'Stable Atmospheric Boundary-Layer Experiment in Spain (SABLES 98) A Report', *Boundary-Layer Meteorol.* **96**, 337–370.

Cuxart, J., Holtslag, A. A. M., Beare, R., Bazile, E., Beljaars, A., Cheng, A., Conangla, L., Ek, M., Freedman, F., Hamdi, R., Kerstein, A., Kitagawa, H., Lenderink, G., Lewellen, D., Mailhot, J., Mauritsen, T., Perov, V., Schayes, G., Steeneveld, G.-J., Svensson, G., Taylor, P., Wunsch, S., Weng, W., and Xu, K. M.: 2006, 'Single-column Model Intercomparison for a Stably Stratified Atmospheric Boundary Layer', *Boundary-Layer Meteorol.*, in press.

Darby, L. S., Banta, R. M., Brewer, W. A., Neff, W. D., Marchbanks, R. D., McCarty, B. J., Senff, C. J., White, A. B., Angevine, W. M., and Williams, E. J.: 2002, 'Vertical Variations in O_3 Concentrations before and after a Gust Front Passage', *J. Geophys. Res.* **107** (D13), 4174, doi 10.1029/2001JD000996.

Deardorff, J. W.: 1980, 'Stratocumulus-capped Mixed Layers Derived from a Three-dimensional Model', *Boundary-Layer Meteorol.* **18**, 495–527.

Holton, J. R.: 1967, 'The Diurnal Boundary Layer Wind Oscillation above Sloping Terrain', *Tellus* **19**, 199–205.

Holtslag, A. A. M.: 2003, 'GABLS Initiates Intercomparison for Stable Boundary Layers', *GEWEX News* **13**, 7–8.

Källstrand, B.: 1998, 'Low Level Jets in a Marine Boundary Layer during Spring', *Contrib. Atmos. Phys.* **71**, 359–373.

Kolmogorov, A. N.: 1942, 'Equations of Turbulent Motion of an Incompressible Fluid', *IZV. Akad. Nauk, SSSR, Ser. Fiz.* **6**, 56–58.

Lafore, J. P., Stein, J., Asencio, N., Bougeault, P., Ducrocq, V., Duron, J., Fisher, C., Héreil, P., Mascart, P., Masson, V., Pinty, J. P., Redelsperger, J. L., Richard, E., and Vilà-Guerau de Arellano, J.: 1998, 'The Meso-NH Atmospheric Simulation System. Part I: Adiabatic Formulation and Control Simulation', *Ann. Geophys.* **16**, 90–109.

Mahrt, L.: 1981a, 'The Early Evening Boundary Layer Transition', *Quart. J. Roy. Meteorol. Soc.* **107**, 329–343.

Mahrt, L.: 1981b, 'Modelling the Depth of the Stable Boundary-Layer', *Boundary-Layer Meteorol.* **21**, 3–9.

Mahrt, L., Heald, R. C., Lenschow, D. H., Stankov, B. B., and Troen, I. B.: 1979, 'An Observational Study of the Structure of the Nocturnal Boundary Layer', *Boundary-Layer Meteorol.* **17**, 247–264.

Mahrt, L., Sun, J., Blumen, W., Delany, T., and Oncley, S.: 1998, 'Nocturnal Boundary-Layer Regimes', *Boundary-Layer Meteorol.* **88**, 255–278.

Mahrt, L. and Vickers, D.: 2003, 'Formulation of Turbulent Fluxes in the Stable Boundary Layer', *J. Atmos. Sci.* **60**(20), 2538–2548.

Parker, M. J. and Raman, S.: 1993, 'A Case Study of the Nocturnal Boundary Layer over a Complex Terrain', *Boundary-Layer Meteorol.* **66**, 303–324.

Pielke, R. A.: 2002, Mesoscale Meteorological Modeling, Academic Press, USA, 676 pp.

Sánchez, E. and Cuxart, J.: 2004, 'A Buoyancy-based Mixing Length Proposal for Cloudy Boundary Layers', *Quart. J. Roy. Meteorol. Soc.*, **130**, 3385–3404.

Smedman, A. S.: 1988, 'Observations of a Multi-Level Turbulence Structure in a Very Stable Atmospheric Boundary Layer', *Boundary-Layer Meteorol.* **44**, 231–253.

Smedman, A. S., Tjernstrom, M., and Högström, U.: 1993, 'Analysis of the Turbulence Structure of a Marine Low-Level Jet', *Boundary-Layer Meteorol.* **66**, 105–126.

Stull, R. B.: 1988, An Introduction to Boundary Layer Meteorology, Kluwer Academic Publishers, Dordrecht, 666 pp.

Terradellas, E. and Cuxart, J.: 2001, Aplicación de un modelo unidimensional para predicciones en el aeropuerto de Madrid-Barajas', V Simposio Nacional de Predicción del INM, Madrid. ISBN: 84-8320-192-5. CD available at Instituto Nacional de Meteorología, Leonardo Prieto Castro, 8, 28040 Madrid, Spain.

Unden, P., Rontu, L., Jarvinen, H., Lynch, P., Calvo, J., Cats, G., Cuxart, J., Eerola, K., Fortelius, C., Garcia- Moya, J. A., Jones, C., Lenderink, G., McDonald, A., McGrath, R., Navascues, B., Nielsen, N. W., Odegaard, V., Rodriguez, E., Rummukainen, M., Room, R., Sattler, K., Saas, B. H., Savijarvi, H., Schreur, B. W., Sigg, R., The, H., and Tijm, A.: 2002, HIRLAM-5 Scientific Documentation, HIRLAM-5 Project, c/o Per Unden SMHI, S-606 76 Norrköping, SWEDEN.

Vukelic, B. and Cuxart, J. 2000, One-dimensional Simulations of the Stable Boundary-layer as Observed in SABLES98', Preprints 14^{th} *Symposium on Boundary Layers and Turbulence*, Aspen, Colorado, August 7–11: 2000, American Meteorological Society, 45 Beacon St., Boston, MA, pp. 579–580.

Whiteman, C. D., Bian, X., and Zhong, S.: 1997, 'Low-level Jet Climatology from Enhanced Rawinsonde Observations at a Site in the Southern Great Plains', *J. Appl. Meteorol.* **36**, 1363–1376.

Wu, Y. and Raman, S.: 1997, 'Effect of Land-use Pattern on the Development of Low-Level Jets', *J. Appl. Meteorol.* **36**, 573–590.

Wu, Y. and Raman, S.: 1998, 'The Summer Time Great Plains Low-Level Jet and the Effect of its Origin on Moisture Transport', *Boundary-Layer Meteorol.* **88**, 445–466.

Zhong, S., Fast, J. D., and Bian, X.: 1996, 'A Case Study of the Great Plains Low-Level Jet using Profiler Network Data and a High-resolution Mesoscale Model', *Mon. Wea. Rev.* **124**, 785–806.